Numerical analysis of a backward flow forming operation of AA6061-T6 and comparison with experiments

Katia Mocellin, M Vidal, F Frascati, P Bouchard

Numerical analysis of a backward flow forming operation of AA6061-T6 and comparison with experiments

K Mocellin[1], M A Vidal[1,2], F Frascati[2] and P O Bouchard[1]

[1] MINES Paris-Tech, PSL- Research University, CEMEF – Center for Material Forming, CNRS UMR 7635, BP 207, 1 rue Claude Daunesse, 06904 Sophia Antipolis Cedex, France

[2] MBDA France, Rond-Point Marcel Hanriot, 18020 Bourges Cedex, France

katia.mocellin@minesparis.psl.eu

Abstract. Incremental forming processes can be used to produce thin products (tubes or sheets)[1]. Very high deformation of the material can be reached taking advantage of the local and cyclic loading of the material. In this study we will focus on backward flow forming of aluminum tubes. In this process, tube thickness is reduced by the combined action of a rotating mandrel that imposes the inner radius and 3 rollers that decrease progressively the tube thickness.

An experimental campaign is conducted on a laboratory device to study the influence of process parameters on tubes formability (rotation speed, feed ratio, reduction rate…). The corresponding configurations are simulated to understand the mechanical loading path. The material characterization is presented to focus on the influence of the chosen behavior law on flow forming simulation results.

Different damage criteria coming from the literature are studied to evaluate their capability to predict fracture and to compare the amount of damage reached for each process configurations.

Introduction

Tube flow forming is an incremental forming process used to produce thin resistant tubes. The incremental loading condition allows the material to reach high deformation without exhibiting fracture. Inner diameter is controlled with a mandrel while thickness is reduced with rotating rollers. Several authors have studied the process from both experimental and numerical point of views [2, 3].

Our objective, in this work, is to develop a numerical model able to understand material loading path, to predict forming forces, geometries and fracture occurrence. We will focus, in this paper in this last part.

To save time and material, a lab scale device is used to study the process rather than an industrial device adapted to large tube dimensions. Smaller tubes are machined in the inner material waste coming from industrial preforms preparation. Geometries of the rollers are defined homothetically from the industrial configuration. Dealing with smaller specimens allows also to reduce the associated CPU time.

Numerical model has to be fed with material behavior laws and damage criteria. The computational model is then used to reproduce an experimental campaign in which increasing reduction ratio is applied

to exhibit the limitation of the process. Three damage models are then evaluated for the prediction of fracture.

1. Material characterization and experimental flow forming campaign

1.1. Material characterization

The behavior of our material was identified using compression tests. Compression samples were extracted from the initial bar along the extrusion direction, in the zone were flow forming tubular preforms were also machined. Localization of both tubes and samples are represented in **Figure 1**. Samples are 12 mm height and 8 mm in diameter.

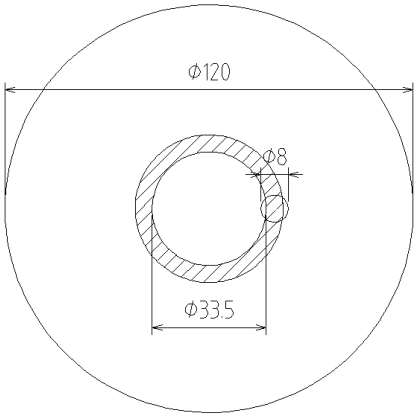

Figure 1. Dimensions of the initial extruded bar from which the flow forming preforms are machined (hachured) and location of the compression samples.

The samples were tested at different strain rates of 0.001, 0.1 and 10 s^{-1} and temperatures, 25, 70 and 100 °C to cover the large range of thermo-mechanical conditions encountered in the flow forming process. Load-displacement curves are shown in

Figure 2. The identification of the parameters of the behavior law was done in three steps using inverse analysis: strain hardening part first, dependence to the temperature and then dependence to strain rate using an in-house software of inverse analysis [4]. Because of self-heating at high strain rate, the dependence to temperature must be identified prior to the dependence to strain rate.

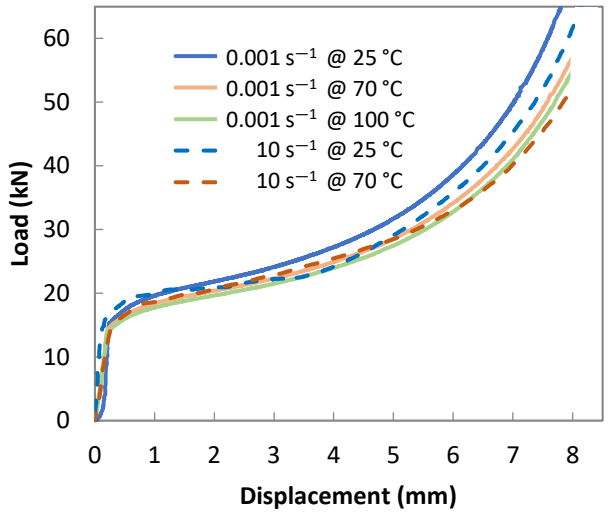

Figure 2. experimental load-displacement curves of compression tests at 0.001 s−1 and 25, 70 and 100 °C (solid lines) and at 10 s−1 at 25 and 70 °C (dotted lines).

The chosen behavior law follows the Johnson-Cook model but with a Voce hardening part as described in equation (1):

$$\sigma = [\sigma_S - (\sigma_S - \sigma_0)\exp(-K\bar{\varepsilon})]\left[1 + C\ln\frac{\dot{\bar{\varepsilon}}}{\dot{\bar{\varepsilon}}_0}\right]\left[1 - \left(\frac{T - T_R}{T_M - T_R}\right)^m\right] \quad (1)$$

σ_0 is the yield stress (MPa), σ_S is the saturated stress (MPa), K is a dimensionless parameter describing the hardening effect, $\bar{\varepsilon}$ is the equivalent plastic strain, C is a dimensionless parameter describing the material sensitivity to strain rate, $\dot{\bar{\varepsilon}}$ is the equivalent strain rate (s^{-1}) of the test, $\dot{\bar{\varepsilon}}_0$ is the strain rate of the reference test (s^{-1}), T is the temperature of the test (°C), T_R is the reference temperature (°C), T_M is the melting point of the material and m is a dimensionless parameter describing the material sensitivity to temperature. The values of the identified parameters for AA6061-T6 alloy using compression tests are summed up in Table 1. This law will be denoted as VJC (Voce and Johnson Cook) law in the following.

Table 1. Identified values using inverse analysis of the parameters of the Voce-Johnson-Cook (VJC) behaviour law for AA6061-T6 tested in compression.

Voce hardening part	Temperature Johnson-Cook part	Strain rate Johnson-Cook part
$\sigma_0 = 301.16\ MPa$	$m = 0.81$	$C = 0.005$
$\sigma_S = 362\ MPa$	$T_R = 25\ °C$	$\dot{\bar{\varepsilon}}_0 = 0.001\ s^{-1}$
$K = 35{,}57$	$T_M = 632\ °C$	

1.2. Experimental flow forming campaign

Flow forming experiments are conducted in CEMEF on a lab sized flow forming machine [5]. It consists on a backward flow forming device with a rotating mandrel. The tubular preform is clamped on at its end and formed with 3 conical rollers. These rollers are arranged at 120° to each other, they are staggered along the Z axis -the revolution axis of the mandrel- and along the thickness of the preform. Each roller takes one third of the total depth (**Figure 3**). The loads can be recorded only on one roller per operation but on all the three directions (radial, tangential and axial).

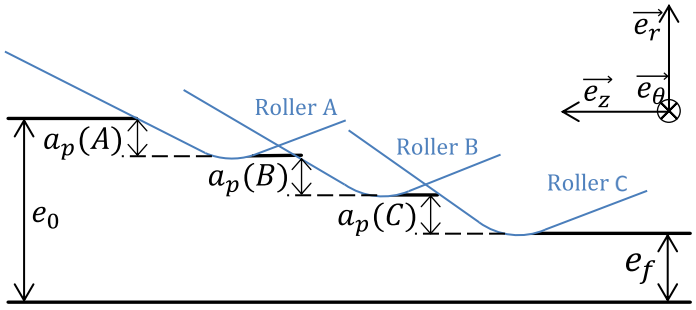

Figure 3.: Illustration of the three rollers staggered along Z if they are represented in the same plane $(\vec{e_r}; \vec{e_\theta})$

An important parameter of the flow forming operation is the reduction ratio or thickness reduction ratio TR(%) which is defined, in this work, by:

$$TR(\%) = 100 \times \frac{e_0 - e_f}{e_o} \quad (2)$$

Where the reduction ratio is expressed in %, $\boldsymbol{e_0}$ is the initial thickness of the preform (mm) and $\boldsymbol{e_f}$ is the final thickness of the tube (mm).

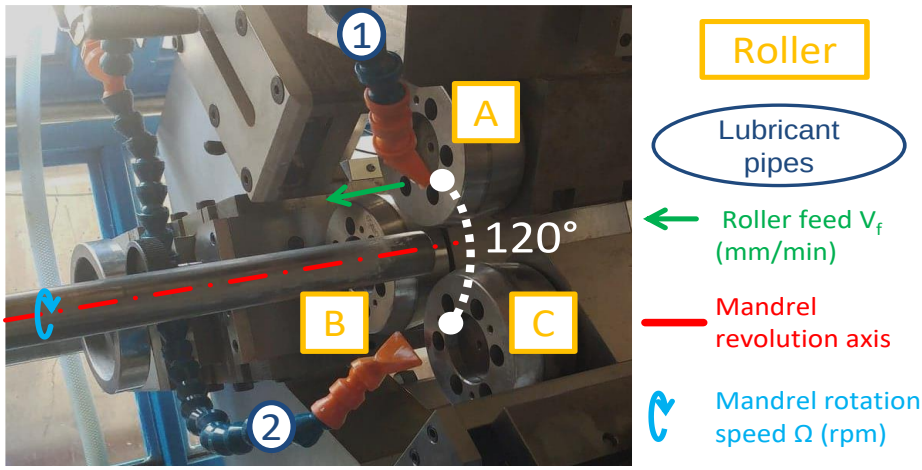

Figure 4. Experimental flow forming device in CEMEF.

For the study of the influence of the behaviour law on tool forces in simulation, we have chosen the following flow forming parameters: a mandrel speed of 50 rpm and an axial feed of 0.2 mm/rotation. Lubrication is performed with intensive flow of water-soluble cutting oil.

For the local analysis of the stress state, four flow forming experiments were conducted at different reduction ratios using the process parameters listed **Table 2**.

Table 2: Denomination and specificity of the experiments used for the local analysis of the stress state during the flow forming operation.

First tube - TR60 1P1	Second tube - TR80 1P1	Third tube- TR80 2P1 and TR80 2P2
One pass of 60% of reduction, $e_0 = 5\ mm$ $e_f = 2\ mm$	One pass of 80% of reduction, $e_0 = 5\ mm$ $e_f = 1\ mm$	First pass (40% of reduction) : TR80 2P1 $e_0 = 5\ mm$ $e_1 = 3\ mm$ Second pass (66.67% of reduction) : TR80 2P2 $e_1 = 3\ mm$ $e_f = 1\ mm$ Achieving 80% of total thickness reduction

In this study, the software Forge® was used. It is based on an implicit formulation with a mixed finite element in velocity and pressure [6]. Forge® is dedicated to the numerical simulation of forming processes implying large deformation. Automatic remeshing and parallel computation can be used to handled large plastic strain in the material and high number of nodes necessary to discretise accurately both the part and the local contact areas [7].

To control the volume variation of the tube during the simulation and to reduce the computation time [8], the description of kinematic interaction is modified. The {mandrel+tube} system is fixed whereas the rollers are rotating around the system at the actual mandrel rotation speed, Ω. The rotation of rollers around themselves due to friction with the tube is fixed during the simulation. The rotation speed is estimated with:

$$\omega_i R_i = \Omega_{mandrel}(R_{mandrel} + e_i) \quad (3)$$

Where $\boldsymbol{i}$ is related either to the roller A, B or C, $\boldsymbol{\omega_i}$ is the roller rotation speed (rpm), $\boldsymbol{R_i}$ is the roller radius (mm), $\boldsymbol{\Omega_{mandrel}}$ is the mandrel rotation speed (rpm), $\boldsymbol{R_{mandrel}}$ is the mandrel radius (mm) and $\boldsymbol{e_i}$ is the tube thickness after the roller $\boldsymbol{i}$ (mm). A global view of the 3D flow forming simulation explaining the specific kinematics is available in **Figure 5** (a).

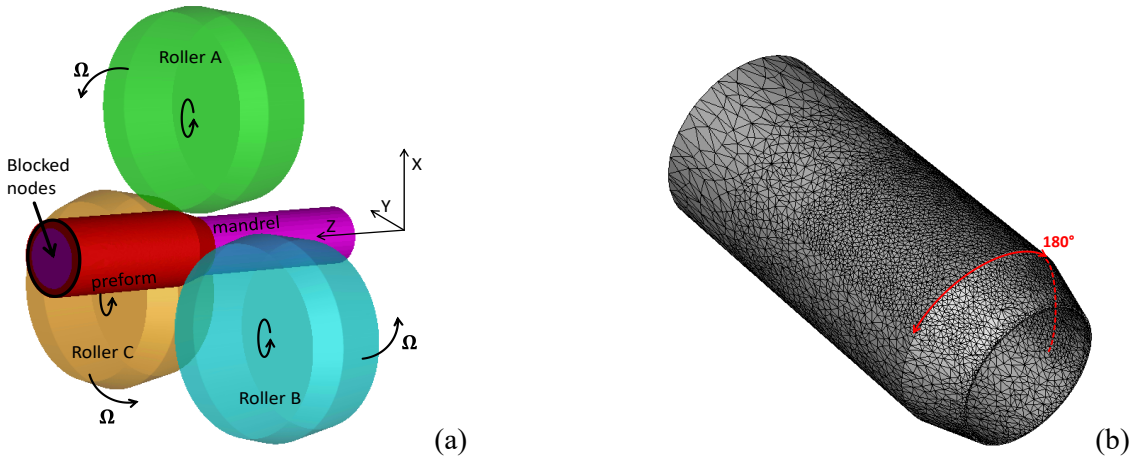

Figure 5: (a) global view of a 3D flow forming simulation using Forge®, (b) Meshed tube used in flow forming simulations in Forge®.

In the flow forming process, the contact zone between the rollers and the tube is very small, thus a small mesh size is required to properly describe the contact events. Moreover, the final thickness of the tube, depending on the reduction ratio, varies from 1 to 2 mm in this study. To capture the difference of stress state along the thickness of the tube, the mesh size is chosen to be lower than the half of the theoretical final thickness. However, having a fine mesh size on the whole tube would lead to very long computation time. To prevent that, only half of the tube is finely meshed as shown in **Figure 5** (b).

Each material point in the flow formed zone of the tube is deformed several times by each roller, at high strain rates and during short contact time, attesting the incremental deformation of the process. Small computation time steps are then required in the simulation, increasing the computation duration of the simulation. The computation time step is arbitrary chosen as half of the time that a roller needs to cover 1° of the tube.

As the tube is lubricated during the experimental flow forming operation, the heat exchange coefficient between the tube and its environment in simulation is set to 2100 $W.m^{-2}.K^{-1}$. The heat exchange coefficient between the tube and the tools is set to 2000 $W.m^{-2}.K^{-1}$. These values are classically used for cold forming lubricated processes.

As the rollers are rotating around themselves due to friction with the tube, a friction coefficient between the tube and the rollers is put in the simulation. A Coulomb-Tresca friction model is used with the respective following parameters: $\mu = 0.2$ and $\bar{m} = 0.4$.

To evaluate the capability to predict fracture of the tubes, damage criteria are computed. Several criteria can be found in the literature for analysis of flow forming [8, 9]. In the following we will focus on the Latham & Cockroft damage depending on the first principal stress, the Oyane based on triaxiality evolution and a variation of the Lou & Huh criterion [10] expressed with respect to local shearing conditions as described in equation (4).

$$D = \int_0^{\varepsilon} \frac{\tau_{max}}{\sigma_{eq}} \, d\bar{\varepsilon} \tag{4}$$

Where D is the damage criterion, τ_{max} is the shearing defined with first and last principal stress components and σ_{eq} the equivalent von Mises stress.

The local mechanical path undergone by the material in flow forming is complex, multiaxial and cyclic. It is then difficult to point out what are the most damaging stress states.

2. Experimental campaign results vs simulation modeling

2.1. Forming forces

Flow forming simulations is compared to experimental results for the 60% of programmed thickness reduction, in the same processing conditions. The forces on the first roller are measured and compared to the simulated ones on **Figure 6**.

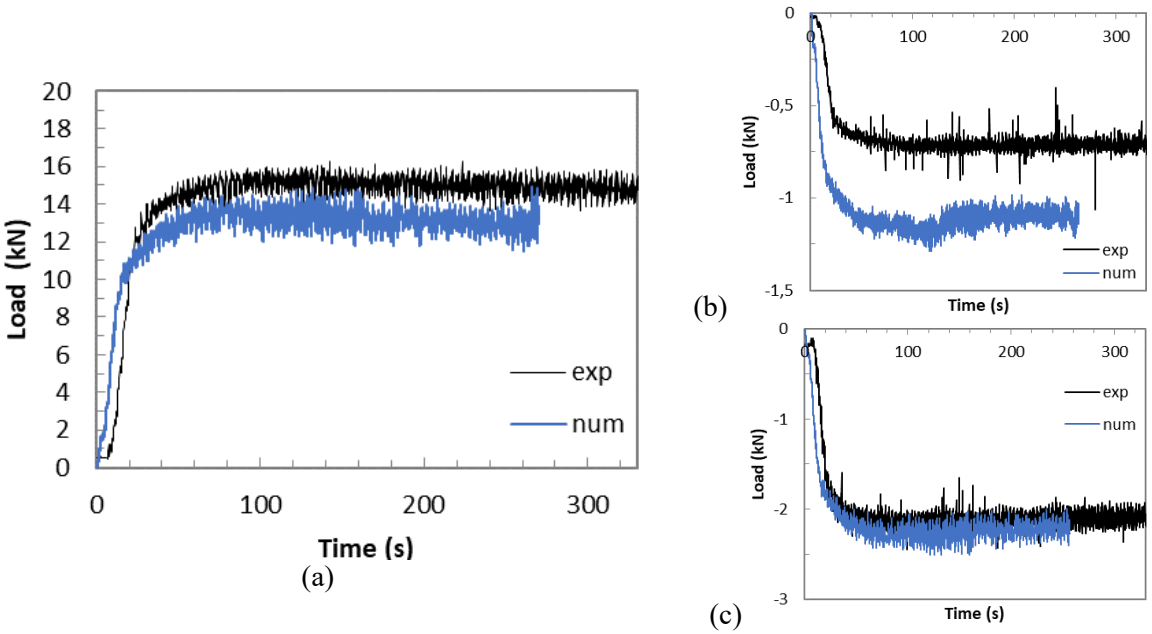

Figure 6. Radial(a), tangential (b) and axial (c) loads on roller A (kN) as a function of process time (s) experimentally and simulated by Forge®.

The force is first increasing when flow forming the conical part and reaching a plateau both in simulation and experimentally.

Radial force is higher than the axial and longitudinal ones. Good agreement is found for the first while small order discrepancies can be found for the 2 others.

2.2. Effect of the reduction ratio

Flow forming forces are recorded on the first roller We will focus on the radial component of the force that is the highest one. The plateau values of radial forces are reported for different reduction ratio in **Figure 7**. The force is increasing with the reduction ratio.

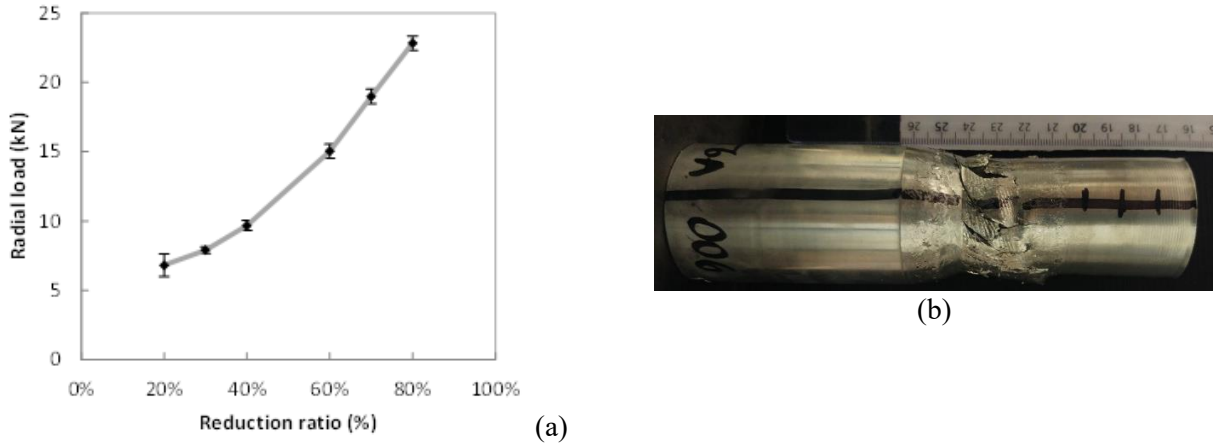

Figure 7. Evolution of forming load with the reduction ratio(a) and fracture observed for 80% TR

The increase of the reduction ratio leads to fracture for 80 % reduction in one step. However, for the third tube the same global reduction ratio is programmed in 2 flow forming steps as mentioned in **Table 2**. This tube didn't show any fracture. Different computed damage criteria are then analyzed on 4

configurations to see which ones can predict the increase of the reduction ratio should lead to an increase of damage and a reduction ratio of 80% leads to more damage when achieved in one pass rather than in two.

2.2.1. Analysis of local mechanical variables

The plastic strain is first analysed on sensors **Figure 8**. One is placed close to the outer surface solicited by the roller, the second close to the inner surface, nearby the mandrel.

The plastic strain is globally higher on the outer surface, values for 80 % (TR801P1) are higher than 60% (TR601P1) and 40% (TR80 2P1) but values for 80 % in 2 passes (TR802P2) is higher than the one for one pass (TR801P1). For 40%, the outer surface is highly deformed, this reduction ratio is not representative of "flow forming" conditions and then difficult to compare with values obtained with higher TR. However,the expected order is respected on the inner face of the tube.

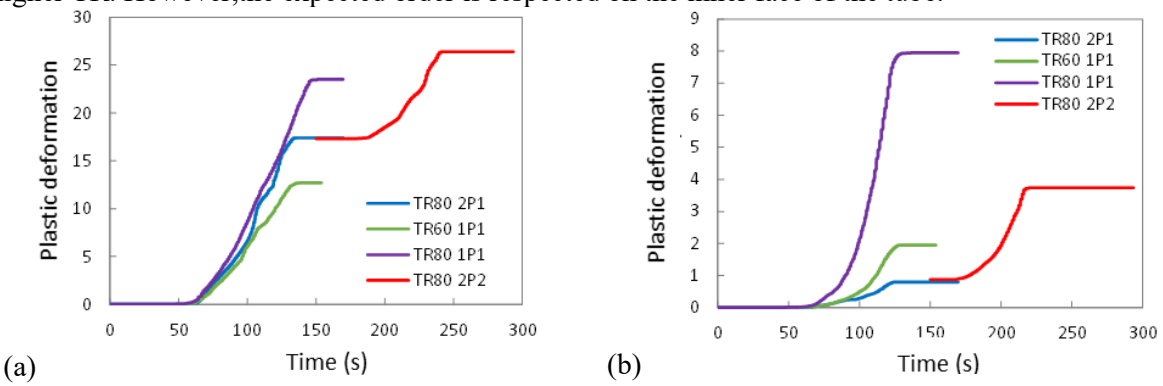

Figure 8. Evolution of plastic strain on sensors placed close to the outer surface (a) or the inner one (b) during flow forming in different configurations

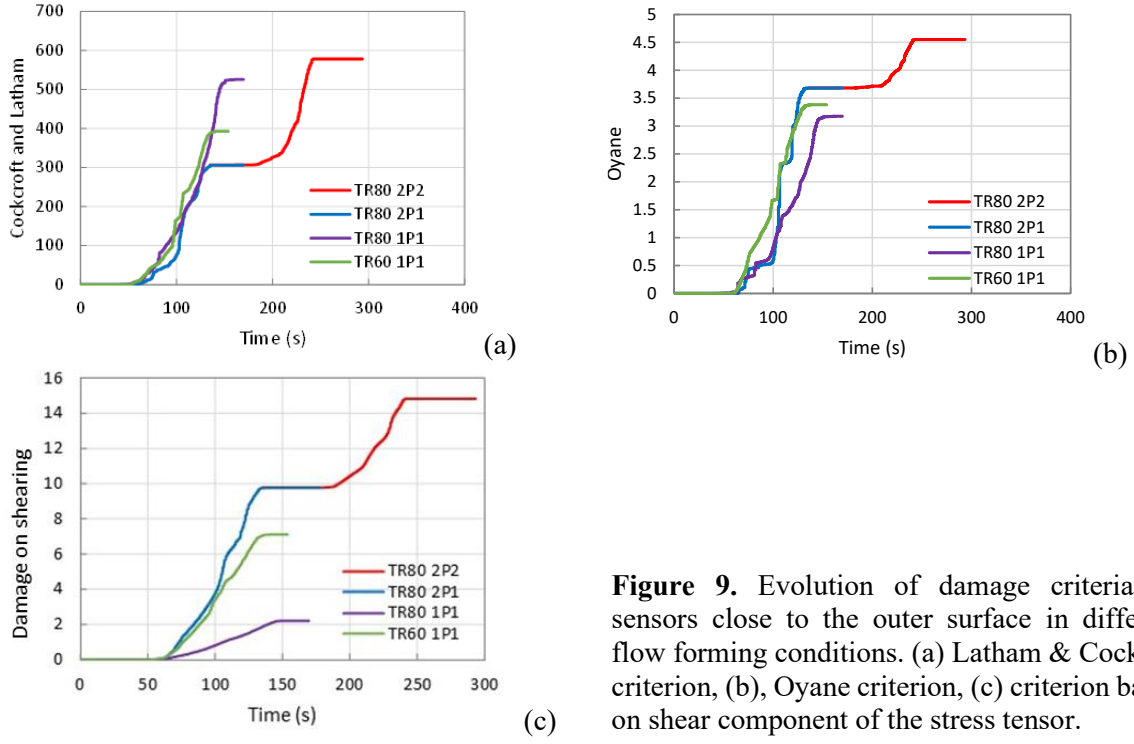

Figure 9. Evolution of damage criteria on sensors close to the outer surface in different flow forming conditions. (a) Latham & Cockroft criterion, (b), Oyane criterion, (c) criterion based on shear component of the stress tensor.

3. Results analysis

Evolution of plastic strain cannot be used to predict fracture as the largest values are located on the outer face of the cylinder and do not follow the expected hierarchy. As a matter of fact, the value recorded for the 2 passes route is higher than the single pass one whereas fracture in observed experimentally in the latest one.

Damage criteria are giving different prediction. Oyane or the shear-based criterion are predicting decreasing damage with increasing reduction ratio. Only the Latham and Cockroft based on the first principal stress and thus the tensile configuration allows to reach the expected hierarchy of the configurations. The difference between the 2 routes of 80 % is however small.

As a conclusion tube flow forming is complex to analyze because the material is incrementally and cyclically deformed reaching values of plastic strain almost impossible to reproduce with standard characterization testing. Classical damage criteria are not giving a clear answer, enhanced formulation must be considered. Mechanical analysis can provide information for the prediction of flow formability, but some metallurgical aspects are neglected in our approach and could help to understand more accurately the capability of the material to be deformed.

References

[1] Music O, Allwood JM, Kawai K-I. A review of the mechanics of metal spinning. *J Mater Process Technol* 2010; 210: 3–23.

[2] Günay E, Fenercioğlu TO, Yalçinkaya T. Numerical analysis of thermo-mechanical behavior in flow forming. *Procedia Struct Integr* 2022; 35: 42–50.

[3] Bylya OI, Khismatullin T, Blackwell P, et al. The effect of elasto-plastic properties of materials on their formability by flow forming. *J Mater Process Technol* 2018; 252: 34–44.

[4] Roux É, Tillier Y, Kraria S, et al. An efficient parallel global optimization strategy based on Kriging properties suitable for material parameters identification. 28.

[5] Depriester D, Massoni E. On the Damage Criteria and their Critical Values for Flowforming of ELI Grade Ti64. *Key Eng Mater* 2014; 622–623: 1221–1227.

[6] Chenot J-L, Bouchard P-O, Fourment L, et al. Numerical Simulation and Optimization of the Forging Process. p. 7 pages.

[7] Coupez T, Digonnet H, Ducloux R. Parallel meshing and remeshing. *Appl Math Model* 2000; 25: p.153.

[8] Ma H, Xu W, Jin BC, et al. Damage evaluation in tube spinnability test with ductile fracture criteria. *Int J Mech Sci* 2015; Complete: 99–111.

[9] Xu W, Wu H, Ma H, et al. Damage evolution and ductile fracture prediction during tube spinning of titanium alloy. *Int J Mech Sci* 2018; 135: 226–239.

[10] Lou Y, Huh H. Prediction of ductile fracture for advanced high strength steel with a new criterion: Experiments and simulation. *J Mater Process Technol* 2013; 213: 1284–1302.